UC Berkeley
UC Berkeley Previously Published Works

Title

Salt-Induced Self-Assembly of Bacteria on Nanowire Arrays

Permalink

Journal

ISSN

Authors

Sakimoto, Kelsey K
Liu, Chong
Lim, Jongwoo
et al.

Publication Date

DOI

Peer reviewed

Salt-induced Self-assembly of Bacteria on Nanowire Arrays

Kelsey K. Sakimoto,[†] *Chong Liu,*[†,‡] *Jongwoo Lim,*[†] *and Peidong Yang*[†,‡,§,*]

[†] Department of Chemistry, University of California, Berkeley, CA 94720, USA

[‡] Materials Sciences Division, Lawrence Berkeley National Laboratory, Berkeley, CA 94720, USA

[§] Kavli Energy Nanosciences Institute, Berkeley, CA 94720, USA

ABSTRACT: Studying bacteria-nanostructure interactions is crucial to gaining controllable interfacing of biotic and abiotic components in advanced biotechnologies. For bioelectrochemical systems, tunable cell-electrode architectures offer a path towards improving performance and discovering emergent properties. As such, *Sporomusa ovata* cells cultured on vertical silicon nanowire arrays formed filamentous cells and aligned parallel to the nanowires when grown in increasing ionic concentrations. Here, we propose a model describing the kinetic and the thermodynamic driving forces of bacteria-nanowire interactions.

KEYWORDS: nanowire, bacteria, self-assembly, alignment, filamentous, DLVO theory

A deeper understanding of the interactions of biological systems with nanostructures has gained pertinence with the development of 1) investigative tools designed to match the micro- to nanometer length scale of single cells,[1,2] as well as 2) hybrid systems which combine the catalytic and synthetic power of microorganisms, such as bacteria, with the optoelectronic capabilities of abiotic materials, such as inorganic nanowires.[3] The majority of the work has been biomedical in nature, devoted to understanding the interface between nanoparticles and mammalian cells as probes of neuronal and eukaryotic cell activity,[4] or to developing nanostructured surfaces designed to prevent the growth of pathogenic bacteria.[5]

In contrast to the chemical and geometric anti-microbial properties desired for applications such as biomedical devices, the growing field of bioelectrochemistry calls for the development of pro-microbial materials to create a controllable and favorable interaction between microorganisms and the surfaces of electrodes.[6,7] The field of bioelectrochemistry has stemmed from the realization that traditional oxidation-reduction reactions, catalysts, and electrodes, can be interchanged with the biochemical reactions and enzymes that drive cellular metabolism. This approach offers the ability to use electrochemistry to both intercept and study the complex chains of biological redox reactions, as well as augment electrochemical systems with the vast synthetic diversity and specificity of enzyme and whole-cell catalysis.[8] In microbial fuel cells (MFCs), bacteria attach to conductive electrodes to catalyze the oxidation of organic matter to generate electricity.[9] In microbial electrosynthesis cells (MECs), external voltage biases are applied to drive the biological reduction of small molecules to synthesize commodity chemicals and fuels.[10] As a first demonstration of a new type of hybrid artificial photosynthesis, we have recently shown that the direct integration of the acetogen *Sporomusa ovata* with high surface area, photoactive silicon (Si) semiconductor nanowires is able to

photoelectrochemically drive the biological reduction of CO_2 to acetate.[3] For such applications, high surface area electrodes, such as carbon cloth or nanostructured electrodes, are desired to increase the performance of typically low density microbial catalysts. Nanowire array photoelectrodes are well suited to such a purpose, providing high photoelectrochemical performance in addition to increased surface area. Advances in these bioelectrochemical systems will be aided first by understanding and controlling the interfacing of bacterium and nanowire.

As an analytical tool, the nanowire array platform offers several distinct advantages to the study of bacteria-surface interactions. With a well-defined geometry, the physical relation between bacteria and nanowire can be precisely measured and analyzed to probe the underlying interaction. By providing a surface perpendicular to the imaging plane, vertically oriented nanowires allow for *in situ* optical monitoring of cell-surface interactions without the need for complex confocal microscopy techniques or other forms of 3D microscopy.[11] For *ex situ* techniques, such as scanning electron microscopy (SEM), the low convective flux through the nanowire array reduces the disruption of cell attachment, guarding against the formation of structural artifacts due to the serial washing and drying steps required for *ex situ* high vacuum techniques. The high surface area allows for quick measurement of many cells at once, enabling quick statistical averaging in order to obtain significant results. These advantages poise nanowire arrays as a potent tool to investigate cell-surface interactions.

Studies of the interactions between cells and nanowires have largely focused on the influence of geometric and steric features of nanowire arrays in cell growth, patterning, and motility.[11–15] By decreasing the spacing between vertical nanowires, bacteria cells can become squeezed and confined into a vertical attachment, parallel to the nanowires.[16] However, cell-nanowire interactions are also greatly influenced by the myriad of environments in which cells

are naturally found. The wide range of temperatures, pH, pressure, and salinity in which microorganisms thrive[17] are liable to alter the surface and colloidal interactions of bacteria and nanostructures,[18] and bears further scrutiny into the role of growth conditions in cell-nanowire interactions.

The approach we have adopted to understand the effect of different growth conditions is to model the interaction between colloids such as bacteria and nanowires by the widely used Derjaguin-Landau-Verwey-Overbeek (DLVO) theory, which describes the pairwise interaction as the sum of a van der Waals attractive force, and an electrostatic repulsive force originating from the pH sensitive, typically negatively charged bacteria membrane and inorganic oxide surface.[19–21] While the attractive force is fairly unalterable, the repulsive force can be readily decreased with increased ionic strength (through increased concentrations of dissolved salts, such as NaCl).[22] While this approach explicitly describes the potential energy landscape of this bacteria-nanowire interaction, dynamic information can be similarly derived,[23] yielding predictive power over the subtle interplay of thermodynamic and kinetic driving forces to attachment. The reduced dimensionality of nanowires and similar length scales to single bacteria cells allow for facile application of one dimensional solutions to DLVO theory, offering a quick and intuitive understanding of this interaction. Such models have been widely used to explain nanoparticle-nanoparticle, protein-protein, and cell-bulk surface interactions,[18,22] and offers a potential route to understanding and tuning bacteria-nanowire interactions.

In this work, we offer the first investigation into the application of nanowire arrays to study the physical interaction between bacteria and nanostructures at varying ionic concentration and pressure. We demonstrate the ability to tune the orientation of attached *S. ovata* cells cultured on Si nanowire arrays of various geometries, employing facile changes in growth

conditions. This offers a generalized approach to study bacteria-nanowire, or more broadly, cell-nanostructure interaction and self-assembly, with applications ranging from bioelectrochemical systems to biomedical control of cell-surface interaction.

To test the validity of our DLVO-based model, Si nanowire arrays were submerged in growth media of varying compositions, inoculated with *S. ovata* cells, and then incubated to simulate the initial electrode colonization by bacteria typical of many bioelectrochemical systems.[3,24] The Si nanowire dimensions (approximately 800 nm in diameter and 25-30 μm in length) were selected in accordance with the optimized geometry for Si photocathode performance (Supporting Information), with the periodicity of the array varied to study the effect of steric confinement. After 6 days of growth, nanowire arrays were removed from the growth media. The resulting bacteria-nanowire structure was analyzed by fluorescence microscopy and scanning electron microscopy (SEM) to quantify the rod-shaped cells' attachment orientations within the array (Supplemental Information, Materials and Methods). When cultured in normal, literature recommended growth media and conditions (~100 mM ionic strength, 100 kPa H_2:CO_2 as growth substrate),[3,10] cross sectional SEM (Fig. 1a) reveals that bacteria populate the array with random orientations with respect to the vertical nanowires. However, when the bacteria are grown on the array in media of increased ionic strength (the normal growth media supplemented with an additional 200 mM NaCl), the cells self-assemble onto the array in a vertically aligned orientation, mostly parallel to the nanowires (Fig. 1b, S1). These results are corroborated by *in situ* fluorescence microscopy, in which (Fig. 1c) unaligned bacteria appear as rods (cells lying flat with respect to the imaging plane, perpendicular to the nanowires), and (Fig. 2d) parallel aligned bacteria appear as circles (a 2 dimensional projection down the length of the bacteria cell). The agreement between *in situ* fluorescence microscope images and *ex situ* SEM images

demonstrates the ability of nanowire arrays to reduce disruptions in cell attachment during preparation for high vacuum techniques. Qualitatively, these results show that increasing the ionic strength by simple addition of NaCl shifts the bacteria-nanowire orientation from a random state (low salt) to a parallel aligned state (high salt).
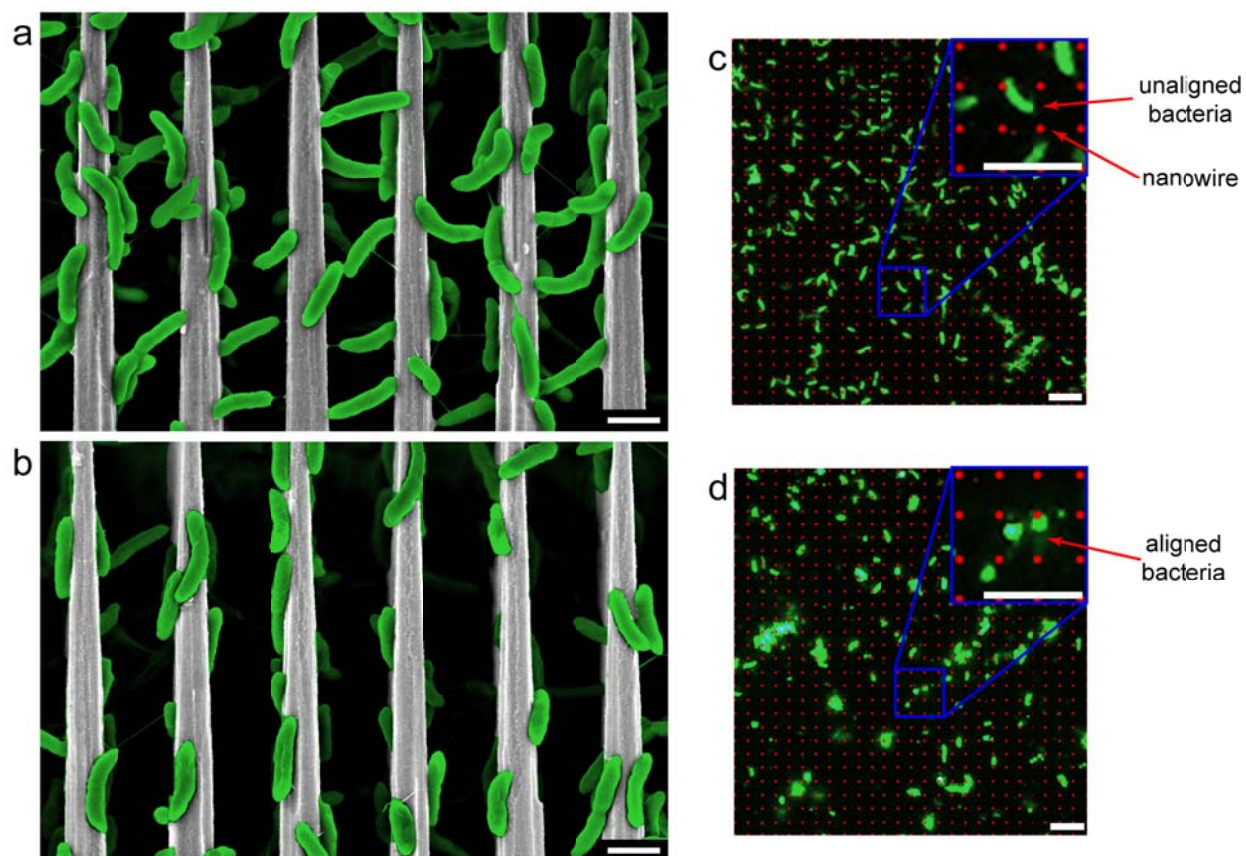

Figure 1. Scanning Electron Microscopy (SEM) and Fluorescence Micrographs of *S. ovata* on Nanowire Arrays. (a,b) SEM and (c,d) fluorescence images were taken of *S. ovata* cells grown on Si nanowire arrays of 4 μm periodicity under (a,c) normal ionic concentrations (~100 mM) and 100 kPa H_2:CO_2, showing random orientations with respect the nanowire axis, and (b,d) with +200 mM NaCl and 500 kPa H_2:CO_2, showing alignment with the nanowire. Both (a,b) side view SEM and (d,e) top down *in situ* fluorescence microscopy show alignment, with (c)

unaligned bacteria appearing as rods in fluorescence micrographs, and (d) aligned bacteria appearing as circles. Scale bars (a,b) 2 μm (c,d) 5 μm.

To further investigate the mechanism of this self-assembled alignment, cell morphology and growth kinetics were measured for planktonic cells under increasing NaCl concentrations to determine whether salt-induced alignment was attributable to physiological changes in the bacteria themselves. Conditions of higher salinity were found to promote cell filamentation, as evidenced by SEM images and broadening of cell length histograms (Fig. 2b,d), regularly producing cells upwards of 2~5 times their normal length. We hypothesized that the observed cell filamentation was attributable to the concomitant increased osmotic pressure produced by addition of NaCl, as has been observed for other bacteria species.[25] . Cell filamentation has been shown to be related to pressure induced inhibition of cell division proteins from either osmotic or hydrostatic pressure changes during growth.[26,27] To test this possibility, *S. ovata* cells were also cultured under conditions of increased hydrostatic pressure up to 500 kPa H_2:CO_2, achieved by pressurizing the headspace above the culture medium. Increased hydrostatic pressure produced similar cell filamentation (Fig. 2c,d). Growth under increased osmotic and hydrostatic pressures were characterized by increased cell doubling times (decreased growth rate) as monitored by cell suspension optical density (Fig. 2e). Filamentous cells were also found to eventually divide into single cells after extended culturing time (>6 days), as well as resist filamentation with the addition of osmolytes such as betaine, which is consistent with previous observations of osmotic and hydrostatic pressure induced arrested cell division and filamentation.[28] Such changes in cell morphology and growth kinetics have the potential to influence cell-nanowire interactions and must be accounted for in subsequent analyses.
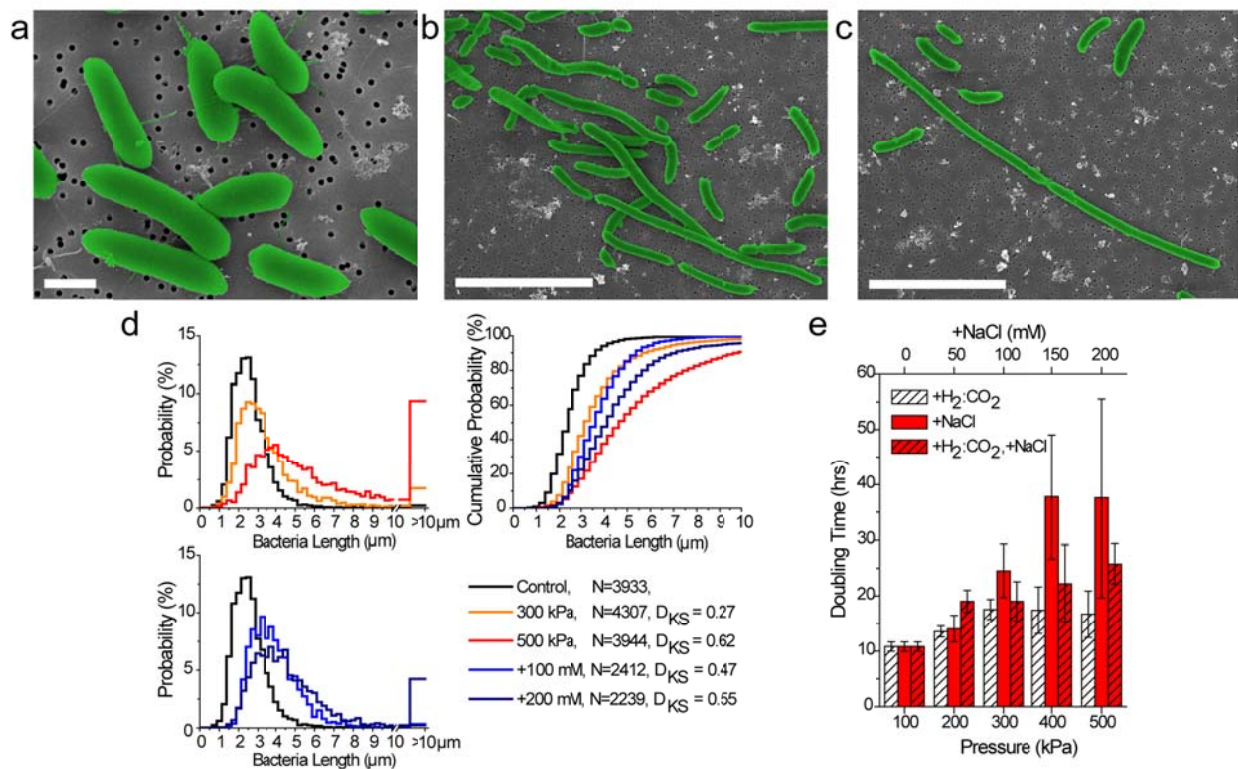
Figure 2. Filamentous Growth of *S. ovata*. (a,d) Under normal growth conditions, *S. ovata* form single cells approximately 2~3 μm x 0.5 μm. With (b,d) increasing NaCl concentrations or (c,d) $H_2:CO_2$ pressure, *S. ovata* forms long filamentous cells. (d) Cell length histograms and two-sample modified Kolmogorov-Smirnov test statistics were calculated, rejecting the null hypothesis at significance α < 0.001.[29] (e) The formation of these filamentous cells is accompanied by increases in the cell doubling time. Scale bars (a) 1 μm, (b,c) 5 μm.

In order to deconvolute the effects of reduced electrostatic repulsion from the effects of cell filamentation brought on by increased ionic strength, cells were cultured on nanowire arrays under conditions of increasing NaCl concentrations, increasing $H_2:CO_2$ pressure, or both. As shown by the radar plots of bacteria-nanowire angles measured from SEM images (Fig. 3), as the

ionic strength is incrementally increased, the distribution of bacteria-nanowire angles gradually shifts from a random (even distribution from 0° to 90°) to a preferentially aligned distribution (large peak centered at 0°). This effect appears to be independent of the previously observed steric control, as square periodic nanowire arrays of both 2 μm and 4 μm periodicity (*S. ovata* diameter ~0.5 μm) display similar trends (Fig. 3, S2). The effect of increasing hydrostatic pressure on bacteria-nanowire orientation was also investigated, and showed minimal variation at the same ionic strength with pressures up to 500 kPa $H_2:CO_2$. The angle distributions were statistically analyzed by means of a two-sample modified Kolmogorov-Smirnov (KS) test.[29] For increasing NaCl concentrations, +100 mM NaCl and +200 mM NaCl, the calculated KS statistic with respect to normal growth conditions similarly increased, rejecting the null hypothesis at a significance of $\alpha < 0.1$ and $\alpha < 0.05$, respectively. Distributions between different nanowire array periodicities and between different pressures showed no statistically significant difference ($\alpha > 0.2$) (Fig. S2). While the effect of cell elongation and retarded growth rate brought on by increased osmotic or hydrostatic pressure cannot be fully discounted, these results suggest that high ionic concentrations alone are required to produce cell alignment.
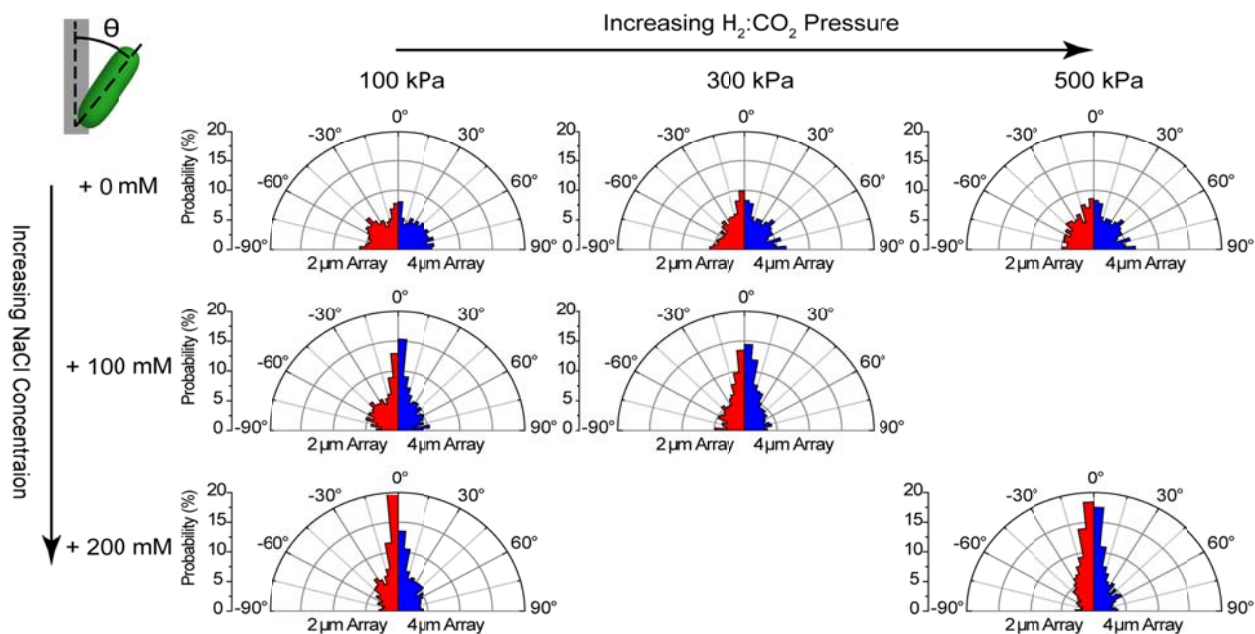
Figure 3. Radar Plots of Bacteria-Nanowire Angle Distribution. Measured angles between bacteria and nanowire axes were measured via SEM for growth conditions of increasing NaCl concentrations, $H_2:CO_2$ pressure, or both. While increasing pressure shows little variation in the angular distribution, increasing NaCl concentrations shows a distinct shift towards the aligned (0°) state.

To provide a mechanistic insight into bacteria-nanowire interactions, DLVO theory interaction energy curves were generated to describe the thermodynamic energy landscape of attachment (Supporting Information, Materials and Methods). Curves were generated for normal ionic concentrations (100 mM total ionic concentration) (Fig. 4a) and +200 mM NaCl conditions (300 mM total ionic concentration) (Fig. 4b), for an unaligned configuration (the bacterium perpendicular to the nanowire, ┼) and an aligned configuration (the bacterium parallel to the nanowire, ‖). While the energies of the primary minima offer insight into the thermodynamic

stability of various configurations, these interactions are influenced not only by thermodynamic factors, but kinetic factors as well.
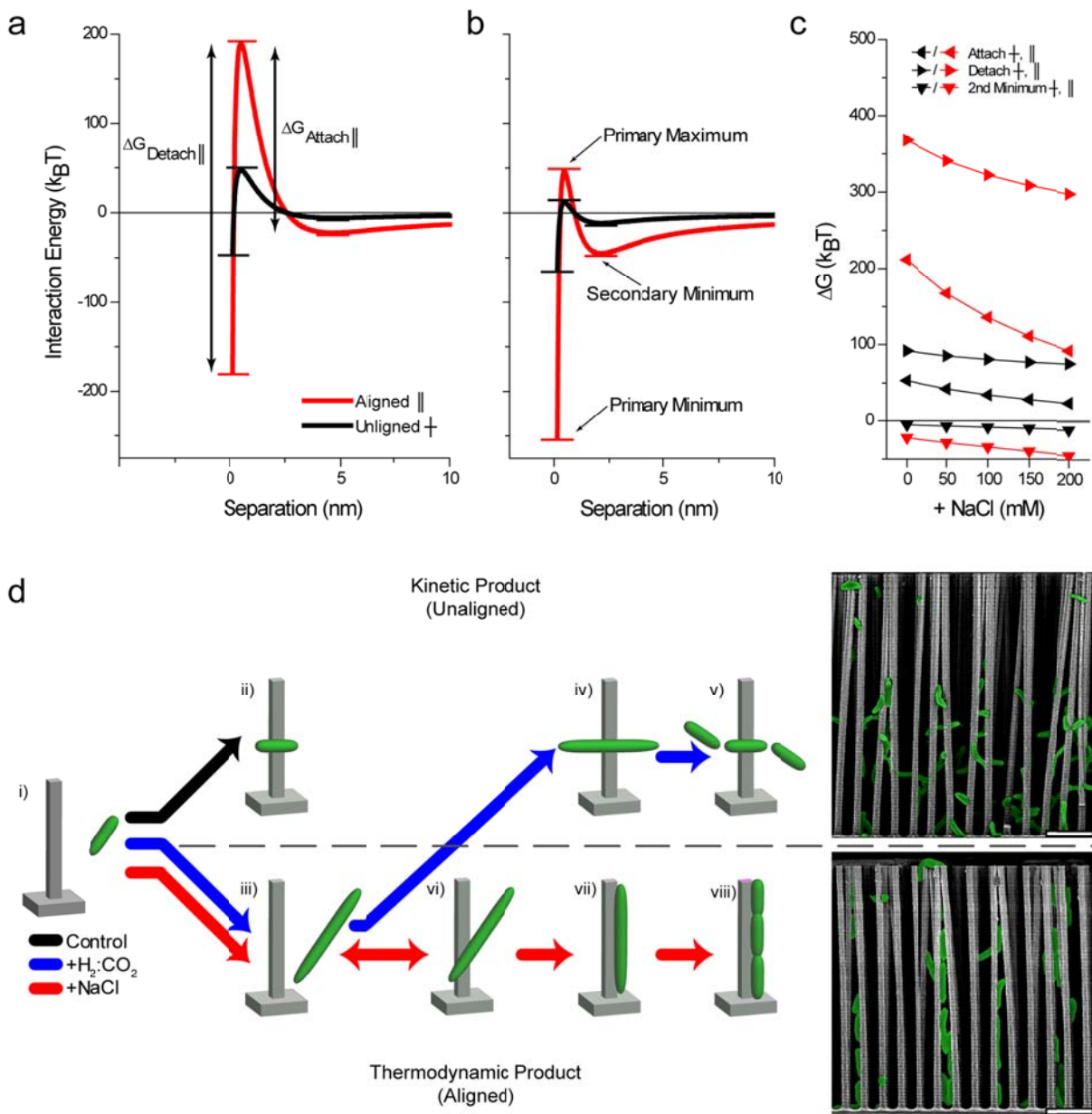

Figure 4. Model and Mechanism of Bacteria-Nanowire Interaction. Derjaguin-Landau-Verwey-Overbeek (DLVO) model curves were generated for bacteria attachment in a perpendicular (unaligned, ╪) and parallel (aligned, ‖) orientation for (a) normal growth conditions and (b)

+200 mM NaCl growth media. (c) The activation energy barriers for attachment, detachment, and the secondary minima were calculated for +0 mM to +200 mM NaCl, showing decreasing values at higher ionic concentrations. d) In the proposed mechanism, i) planktonic cells ii) attach in the unaligned state (kinetic product) under normal conditions. Under increased hydrostatic or osmotic pressure iii) filamentous cells form. At normal ionic strengths, iv-v) the kinetically favored unaligned state is achieved. However, at increasing NaCl concentrations, vi) the bacteria cell enters a reversible adhesion state, from which vii-viii) the thermodynamically favored product is achieved. Representative SEM images for *S. ovata* grown at (top) control conditions and +200 mM NaCl (bottom) on 2 μm periodicity arrays are included. Scale bars 5 μm.

The bacteria-nanowire angle distribution was rationalized in terms of the kinetic rates of attachment and detachment for each configuration. From this, the angle distribution will shift towards the configuration pathway with a faster effective rate (i.e. the sum of attachment and detachment rates). Analogous to transition state theory for chemical reactions, the rate of attachment/detachment is exponentially proportional to the height of the activation energy barrier, $\Delta G_{attach/detach}$ (Fig. 4a).[23] At normal ionic concentrations, the aligned configuration pathway is relatively slow due to the large energy barrier ($\Delta G_{attach,\parallel} >> \Delta G_{attach,+}$). As such, the kinetically favored pathway with the smaller energy barrier is achieved, disfavoring bacteria-nanowire alignment.

Due to the decreasing electrostatic repulsion with increasing ionic strength, all free energies decrease under high salt conditions (Fig. 4c).[18,22] As the ionic strength increases from 100 mM to 300 mM (+0 mM to +200 mM NaCl), the heights of both the aligned and unaligned

pathway energy barriers decrease. In the unaligned pathway, $\Delta G_{\text{attach},+}$ is comparable in magnitude to $\Delta G_{\text{detach},+}$, meaning this pathway is fairly reversible. In contrast, $\Delta G_{\text{attach},\parallel} \ll \Delta G_{\text{detach},\parallel}$, indicating parallel attachment is still fairly irreversible. Thus, at this high ionic strength, the bacteria become trapped in the orientation with the lowest primary minimum, selecting the thermodynamically favored attachment scheme (alignment). Also notable is the formation of a pronounced secondary minimum, allowing the cell to loosely associate with the nanowire in a reversible attached state, from which the bacteria can sample several possible attachment configurations, and come to rest in the most energetically favorable one.[30]   Though elongation produced by increases in hydrostatic pressure alone is unable to effect bacteria-nanowire alignment, the effect of cell elongation under increased ionic strength (increased osmotic pressure) cannot be wholly discounted. As cells elongate under increased osmotic pressure, the thermodynamic driving force and concomitant torque force towards alignment become magnified, scaling with cell surface area. Additionally, previous work has suggested attachment efficiency is also mediated by cell growth phase.[31] Due to cell membrane surface charge heterogeneities during the early stages of growth, electrostatic repulsion is reduced, allowing faster adhesion rates. The observed preferential alignment perhaps stems in part from the longer growth time scale under increased osmotic pressures (Fig. 2e).   From these observations, a mechanism for bacteria-nanowire interactions is proposed (Fig. 4d).

Our results have demonstrated the ability to control the orientation of bacteria attachment to nanowires by simple changes in ionic strength, utilizing nanowire arrays as a platform for precise measurement of cell-surface attachment. More generally, the applicability of DLVO theory towards cell-nanostructure interactions demonstrated by this work provides a well-studied

predictive framework for not only investigations of bioelectrochemical systems, but for the further development of nanomaterials for the biomedical and biotechnological fields, where widely varying temperatures, pressures, pH, salinities and surface properties are regularly encountered. As we have shown, this predictive power enables both the analysis of and the ability to modulate the subtle interplay of thermodynamic and kinetic driving forces to control this colloidal interaction. These insights into the fundamental nature of bacteria-nanowire interactions offer a path towards designing the next generation of nano-bio hybrid systems.

ASSOCIATED CONTENT

Supporting Information Available: Additional figures, materials and methods. This material is available free of charge via the Internet at http://pubs.acs.org.

AUTHOR INFORMATION

Corresponding Author

*To whom correspondence should be addressed: p_yang@berkeley.edu

REFERENCES

(1)   Yan, R.; Park, J.-H.; Choi, Y.; Heo, C.-J.; Yang, S.-M.; Lee, L. P.; Yang, P. *Nat. Nanotechnol.* **2012**, *7*, 191–196.

(2) Gómez-Hens, A.; Fernández-Romero, J. M.; Aguilar-Caballos, M. P. *Trends Anal. Chem.* **2008**, *27*, 394–406.

(3) Liu, C.; Dasgupta, N., Sakimoto, K. K.; Yang, P. Program—Symposium D8.15: Materials for Photoelectrochemical and Photocatalytic Solar-Energy Harvesting and Storage, MRS Spring meeting, San Francisco, 2014.

(4) Hanson, L.; Lin, Z. C.; Xie, C.; Cui, Y.; Cui, B. *Nano Lett.* **2012**, *12*, 5815–5820.

(5) Friedlander, R. S.; Vlamakis, H.; Kim, P.; Khan, M.; Kolter, R.; Aizenberg, J. *Proc. Natl. Acad. Sci. U. S. A.* **2013**, *110*, 5624–5629.

(6) Wang, H.; Ren, Z. J. *Biotechnol. Adv.* **2013**, *31*, 1796–1807.

(7) Zhang, T.; Nie, H.; Bain, T. S.; Lu, H.; Cui, M.; Snoeyenbos-West, O. L.; Franks, A. E.; Nevin, K. P.; Russell, T. P.; Lovley, D. R. *Energy Environ. Sci.* **2013**, *6*, 217–224.

(8) *Bioelectrochemical Systems: From Extracellular Electron Transfer to Biotechnological Applications*; Rabaey, K.; Angenent, L.; Schroder, U.; Keller, J., Eds.; IWA Publishing: London, 2010.

(9) Logan, B. E. *Nat. Rev. Microbiol.* **2009**, *7*, 375–381.

(10) Nevin, K. P.; Woodard, T. L.; Franks, A. E.; Summers, Z. M.; Lovley, D. R. *MBio* **2010**, *1*, e00103–10.

(11) Jeong, H. E.; Kim, I.; Karam, P.; Choi, H.-J.; Yang, P. *Nano Lett.* **2013**, *13*, 2864–2869.

(12) Qi, S.; Yi, C.; Ji, S.; Fong, C.-C.; Yang, M. *ACS Appl. Mater. Interfaces* **2009**, *1*, 30–34.

(13) Epstein, A. K.; Hochbaum, A. I.; Kim, P.; Aizenberg, J. *Nanotechnology* **2011**, *22*, 494007.

(14) Männik, J.; Driessen, R.; Galajda, P.; Keymer, J. E.; Dekker, C. *Proc. Natl. Acad. Sci. U. S. A.* **2009**, *106*, 14861–14866.

(15) Anselme, K.; Davidson, P.; Popa, A. M.; Giazzon, M.; Liley, M.; Ploux, L. *Acta Biomater.* **2010**, *6*, 3824–3846.

(16) Hochbaum, A. I.; Aizenberg, J. *Nano Lett.* **2010**, *10*, 3717–3721.

(17) Van den Burg, B. *Curr. Opin. Microbiol.* **2003**, *6*, 213–218.

(18) Norde, W. *Colloids and Interfaces in Life Sciences and Bionanotechnology*; 2nd ed.; CRC Press, Taylor & Francis Group: Boca Raton, FL, 2011.

(19)   Li, B.; Logan, B. E. *Colloids Surfaces B Biointerfaces* **2004**, *36*, 81–90.

(20)   Bayoudh, S.; Othmane, A.; Mora, L.; Ben Ouada, H. *Colloids Surf. B. Biointerfaces* **2009**, *73*, 1–9.

(21)   Rijnaarts, H. H. M.; Norde, W.; Lyklema, J.; Zehnder, A. J. B. *Colloids Surfaces B Biointerfaces* **1999**, *14*, 179–195.

(22)   Eastman, J. In *Colloid Science: Principles, methods and applications*; Cosgrove, T., Ed.; Blackwell Publishing Ltd: Oxford, 2005; pp. 36–49.

(23)   Elimelech, M. *Water Res.* **1992**, *26*, 1–8.

(24)   Ramasamy, R. P.; Ren, Z.; Mench, M. M.; Regan, J. M. *Biotechnol. Bioeng.* **2008**, *101*, 101–108.

(25)   Csonka, L. N. *Microbiol. Rev.* **1989**, *53*, 121–147.

(26)   Ishii, A.; Sato, T.; Wachi, M.; Nagai, K.; Kato, C. *Microbiology* **2004**, *150*, 1965–1972.

(27)   Kawarai, T.; Furukawa, S.; Narisawa, N.; Hagiwara, C.; Ogihara, H.; Yamasaki, M. *J. Biosci. Bioeng.* **2009**, *107*, 630–635.

(28)   Meury, J. *Arch. Microbiol.* **1988**, *149*, 232–239.

(29)   Stephens, M. A. *J. R. Stat. Soc. Ser. B* **1970**, *32*, 115–122.

(30)   Poortinga, A. T.; Bos, R.; Busscher, H. J. *Langmuir* **2001**, *17*, 2851–2856.

(31)   Walker, S. L.; Hill, J. E.; Redman, J. A. *Appl. Environ. Microbiol.* **2005**, *71*, 3093–3099.

TOC Graphic